Desalination and Water Treatment
www.deswater.com

doi: 10.5004/dwt.2017.20407

65 (2017) 89–97
February

Treatment of anaerobic membrane bioreactor (AnMBR) effluent using direct contact membrane distillation

Lin Chen[a,b,*], Chang Liu[b], Chuqing Cao[c], Liang Zhu[a,b]

[a]*Key Laboratory of Integrated Regulation and Resources Development of Shallow, Lakes, Hohai University, Nanjing 210098, China, emails: chen_lin@hhu.edu.cn (L. Chen), 1745988750@qq.com (L. Zhu)*
[b]*College of Environment, Hohai University, Nanjing 210098, China, email: flying_23@163.com (C. Liu)*
[c]*School of Mechanical Engineering, Nanjing University of Technology and Science, Nanjing 210000, China, email: caochuqing0102@163.com*

Received 28 March 2016; Accepted 7 December 2016

ABSTRACT

This study was conducted using a direct contact membrane distillation (MD) to treat effluent from an anaerobic membrane bioreactor (AnMBR) through a polytetrafluoroethylene (PTFE) membrane. The decrement of membrane flux, and the changes of feed and distillate characteristics were investigated during the production of demineralized water. In general, membrane flux decreased from 9.5 to 3.8 L/m^2/h, and the conductivity in the feed side increased from 1.0 to ~17.5 mS/cm within a time interval of approximately 15 d, while the distillate electrical conductivity was quite stable in a range of 0.09–0.15 mS/cm. Additionally, the results showed that MD exhibited good separation of the AnMBR effluent for non-volatile organics (e.g., protein, polysaccharides), phosphate, and metal ions, but limited effectiveness for volatile foulants such as ammonia. The rejection rate for chemical oxygen demand and phosphate was greater than 98%, but ammonia easily passed through the micro-porous membrane with a final concentration of 6.8–15.7 mg/L in the permeate. Most importantly, the membrane permeate could be recovered to 94% of the initial flux with 0.8 wt% citric acid and 0.3 wt% HCl cleaning for each run, and the module performance was restored to near the initial efficiency, suggesting the feasibility of MD for the treatment of wastewater effluent in a relatively long operation time. Finally, the morphology and composition of the fouling layer were studied, and it was found that salt crystallization resulting in $CaCO_3$ precipitation was determined as a key problem of demineralized water production.

Keywords: Membrane distillation; AnMBR effluent; Long-term performance; Treatment efficiency; Membrane fouling

1. Introduction

In recent years, there has been increasing pressure for water reuse for industrial and municipal purposes leading to the development of mutually beneficial technologies, such as membrane-based separation [1]. Membrane processes are presently being applied for the treatment of municipal and industrial wastewater, the removal of organics and inorganics from (under)ground water, and the desalination of seawater and brackish water [2,3]. However, most membrane separation processes are operated under isothermal conditions relying on the force from hydrostatic pressure differences (such as reverse osmosis [RO] and nano-filtration). One limitation during the pumping cycle has been the high energy requirement for a hydraulic-driven membrane; therefore, there is a significant need to develop technologies with improved interception and lower energy consumption.

Recent achievements in membrane technology and the increased focus on the renewable energy resource exploitation suggested that emerging membrane distillation (MD) technology may be an effective and efficient alternative to conventional membrane processes for water reclamation and

* Corresponding author.

seawater desalination [2,3]. MD technology is a thermally driven process that combines conventional distillation and membrane separation, wherein the water from the feed side is heated to increase its vapor pressure, generating a difference in the partial pressure on each side of the membrane [2]. The membrane acts as an effective barrier for the separation of water and vapor, only allowing vapor molecules to pass through the micro-porous hydrophobic membrane. The MD showed better water quality and remarkable removal efficiency for salts and phosphate. Additionally, due to the absence of hydraulic pressures, MD showed less fouling treatment compared with pressure-driven process. A renewable energy generator, such as wind or solar power or a waste energy recovery system, could also be employed for alternative energy production for MD operation [4], allowing more widespread application.

Because of these potential advantages, there has been increased focus on the continued development of MD for wastewater treatment with acceptable membrane flux and high removal efficiency for organics/inorganics. Presently, MD has been successfully applied in brines reclamation [5,6], water desalination [2], fruit juice concentration [7], and other industrial areas [8,9] at both the lab scale and pilot plant scale. Kim et al. [10] investigated the efficacy of different materials in the application of the MD process for post-treatment of anaerobic bioeffluent for 150 h. Liu and Wang [11] studied effects of operating parameters including feed temperature, feed velocity, and feed concentration for the MD process treatment of low-level radioactive wastewater. Jacob et al. [12] evaluated the effect of biomass on the flux and fouling interaction on MD for treating effluent in a batch mode. There have been only few reports describing use of the MD process for the treatment of effluent from aerobic/anaerobic membrane reactor [10,12], and no consideration was given to the fouling layer on the membrane surface. Additionally, most published work of MD processes described relatively short-time membrane performance, and few studies were of longer time period, such as several weeks including membrane cleaning during operation.

Here, the relatively long-term performance of lab-scale MD fed with an anaerobic membrane bioreactor (AnMBR) effluent was studied comprehensively to examine effects of membrane flux, conductivity changes, nutrient removal, and organics rejection. Simultaneously, the characteristics of feed with operation time were investigated using a three-dimensional excitation–emission matrix (EEM). Finally, the fouling layer was studied by attenuated total reflectance Fourier transform infrared (ATR-FTIR) and scanning electron microscopy (SEM) coupled with energy-dispersing spectrometry (EDS).

2. Materials and methods

2.1. Direct contact membrane distillation configuration

Fig. 1 shows a schematic diagram of the experimental setup. Hydrophobic polytetrafluoroethylene (PTFE) flat sheet membrane with a nominal pore size of 0.22 μm was used. Chlorinated polyvinyl chloride material with temperature tolerance up to 90°C was used for module fabrication. Flow path cavities on both sides of the membrane allowed feed and permeate flows. The feed and permeate stream from the membrane module were circulated in a counter-flow pattern by peristaltic pumps with a cross-flow rate of 10.5 mm/s, and the temperature was controlled at 70°C and 25°C using a heater and a cooler, respectively. The peristaltic pump for the influent was controlled by a water level sensor in the feed side to maintain a constant water volume around 400 mL. The membrane flux was derived by mass balance accounting for the membrane area, and then normalized for clean membrane flux. In the later stage of the studies, the fouled membrane was immersed in 0.8 wt% citric acid solution for 4 h and then 0.3 wt% HCl for 2 h. After cleaning, the membrane was rinsed with tap water and dried overnight. Subsequently, the experiment was resumed with the cleaned membrane and fresh feed.

The feed for the MD process was collected from the effluent of an AnMBR. With an influent chemical oxygen demand (COD) of about 1,100 mg/L for the AnMBR setup, the COD removal efficiency was excellent and stable with an average over 90% at the investigated hydraulic retention time (7 h), and the effluent COD was in a range of 76–93 mg/L. Additionally, the detailed information for the effluent used as the MD feed is listed in Table 1.

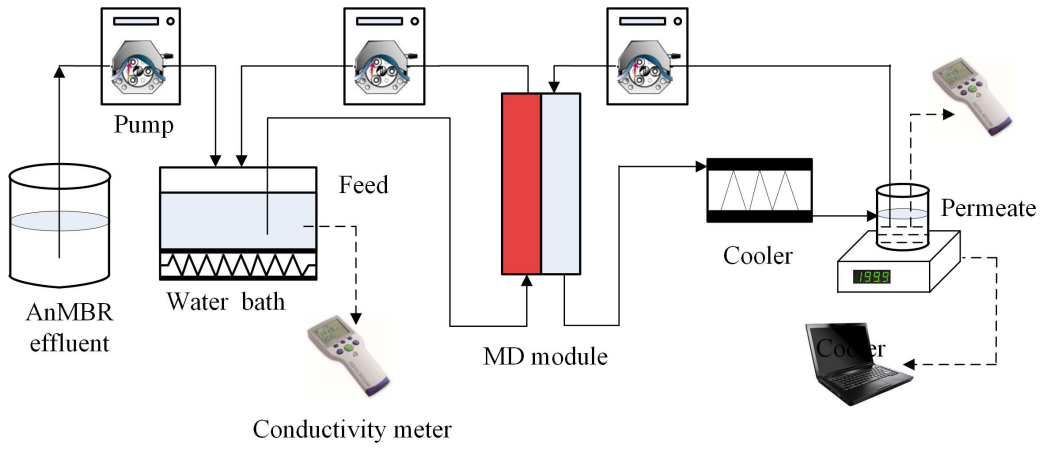

Fig. 1. Schematic diagram of the MD system.

Table 1
Characteristics of AnMBR effluent

Parameter	AnMBR effluent
pH	6.8 ± 0.1
Conductivity (mS/cm)	0.9 ± 0.1
COD (mg/L)	81.6 ± 13.4
NH_4^+–N (mg/L)	33.2 ± 1.7
PO_4^{3-}–P (mg/L)	2.3 ± 0.3
VFA (mg/L)[a]	17.9 ± 4.5
Protein (mg/L)	17.5 ± 2.6
Polysaccharides (mg/L)	3.1 ± 1.2

[a]VFA presented as COD concentration: VFA (as COD) = 0.35 (formate) + 1.07 (acetate) + 1.51 (propionate) + 1.82 (butyrate + isobutyrate) + 2.04 (valerate + isovalerate).

2.2. Analytical methods

During MD operation, samples were taken daily for analysis. The performance was evaluated by permeate flux, and the interception of non-volatile component in the MD process was defined according to the following expression (Eq. (1)):

$$R_s = \left(1 - \frac{C_{permeate}}{C_{feed}}\right) \times 100\% \quad (1)$$

where R_s, $C_{permeate}$ and C_{feed} are interception rate, concentration in permeate side and concentration in feed side, respectively.

COD, ammonia concentration (NH_4^+–N), and phosphate (PO_4^{3-}) were determined using potassium dichromate method, Nessler's reagent colorimetry, and ascorbic acid ammonia molybdate spectrophotometric method, respectively [13]. The conductivity and pH were analyzed by conductivity meter (DDS-11A, Shengci Technology Co., Beijing, China) and pH meter (U8-10, Denver Instrument Company, Arvada, CO, USA), respectively.

The carbohydrates and proteins were analyzed using the phenol–sulfuric acid method [14] and modified Lowry method [15], respectively. EEM spectroscopy (LS55, PerkinElmer, Norwalk, CT, USA) was applied to characterize the changes in the feed and permeate side with operation time. ATR-FTIR (TENSOR 27, Bruker Optik, Ettlingen, Germany) spectroscopy was employed to identify the functional groups that correlated with membrane fouling. Additionally, the morphology of the fouling layer on the membrane surface was evaluated by SEM (S-488, Hitachi Co., Japan) coupled with EDS (Octane plus, AMETEK, Inc., USA).

3. Results and discussion

3.1. Flux performance, pH changes, and salt accumulation

The performance of the MD system is evaluated for distillate flux, liquor conductivity, and pH, as demonstrated in Figs. 2(a)–(c). In general, membrane flux decreased from 9.5 to 3.4 L/m^2/h (LMH), the conductivity in the feed side increased from 1.0 to ~17.5 mS/cm, and pH increased to 10.2 within a time interval of approximately 15 d (1 cycle).

To better show this progression, a period from day 1 to day 15 (cycle I) is described in detail. The relative membrane flux linearly decreased to nearly 0.7 over the first 6 d, then decreased at a faster pace until day 9, at which point the rate slowed down to 0.15–0.26 LMH per day. The permeability decreased with the operation time and reduced by 60%–70% at the end of each run, likely due to membrane fouling (scaling) associated with the growing substance concentration in the feed side. The reduction of membrane permeability resulted from membrane fouling, in which deposit formed on the membrane surface and/or within its pores, decreasing the effective area of the membrane surfaces and also changing the temperature polarization [16]. The deposit layer of suspended or dissolved substances increased the thermal resistance, reducing the heat transfer coefficient from the bulk phase to the evaporation and condensation surfaces as the temperature polarization increased. Hence, the driving force for mass transfer decreased, and membrane flux decreased dramatically. Gryta [17] found that the formation of a non-porous layer led to increased mass transfer resistance and the value of the permeate flux approached zero in an exponential manner. Additionally, the rate of crystallization may have increased as the feed water became more concentrated (with a higher concentration of barely soluble salts) and the number of seed crystals reached the threshold for rapid growth on the membrane surface [18], thus accelerating the reduction of membrane permeability.

After 1 cycle (about 15 d) operation, the membrane was chemically washed, and the solution in the feed side was discharged. The membrane flux was significantly recovered and reached 94% of the initial flux (day 16: flux = 9.38 LMH; day 31: flux = 9.35 LMH), likely due to the improved smooth membrane surface, suitable membrane pore size, and absence of internal fouling. Such significant recovery level suggested that MD systems are highly effective for long-term usage in water treatment, and further research to improve technology for anti-scaling and to reduce salt accumulation is warranted.

Fig. 2(b) illustrates the electrical conductivity in the feed and permeate side throughout the study. The distillate electrical conductivity was quite stable in a range of 0.09–0.15 mS/cm, suggesting a high retention of inorganic solutes up to 99.7%. This retention occurred despite the presence of high salt concentrations in the feed and regular membrane cleaning throughout the study. These results showed that the leakage of the feed through the membrane or serious membrane wetting did not occur during operation, suggesting the efficacy of this process for water reuse.

The pH in the feed side increased with operation time to reach 10.0 at the end of each run as that in the permeate side decreased to around 6.7. The increased pH in the feed side might indicate that the alkaline ions (e.g., HCO_3^-, CO_3^{2-}) were effectively retained by the membrane and concentrated to a higher degree. At the same time, the HCO_3^- ions underwent decomposition to produce CO_3^{2-} with heating ($2HCO_3^- \rightleftarrows CO_3^{2-} + CO_2 + H_2O$) [19]. Additionally, the vapor pressures of volatile fatty acids (VFAs), CO_2, and ammonia were many orders of magnitude higher than that of water molecules, allowing these compounds to partially pass through the membrane and alter the permeate pH.

3.2. MD treatment for AnMBR effluent

3.2.1. COD variation and rejection efficiency

The variation of COD in the feed side and distillate is shown in Fig. 3(a). Only a slight amount of COD, below

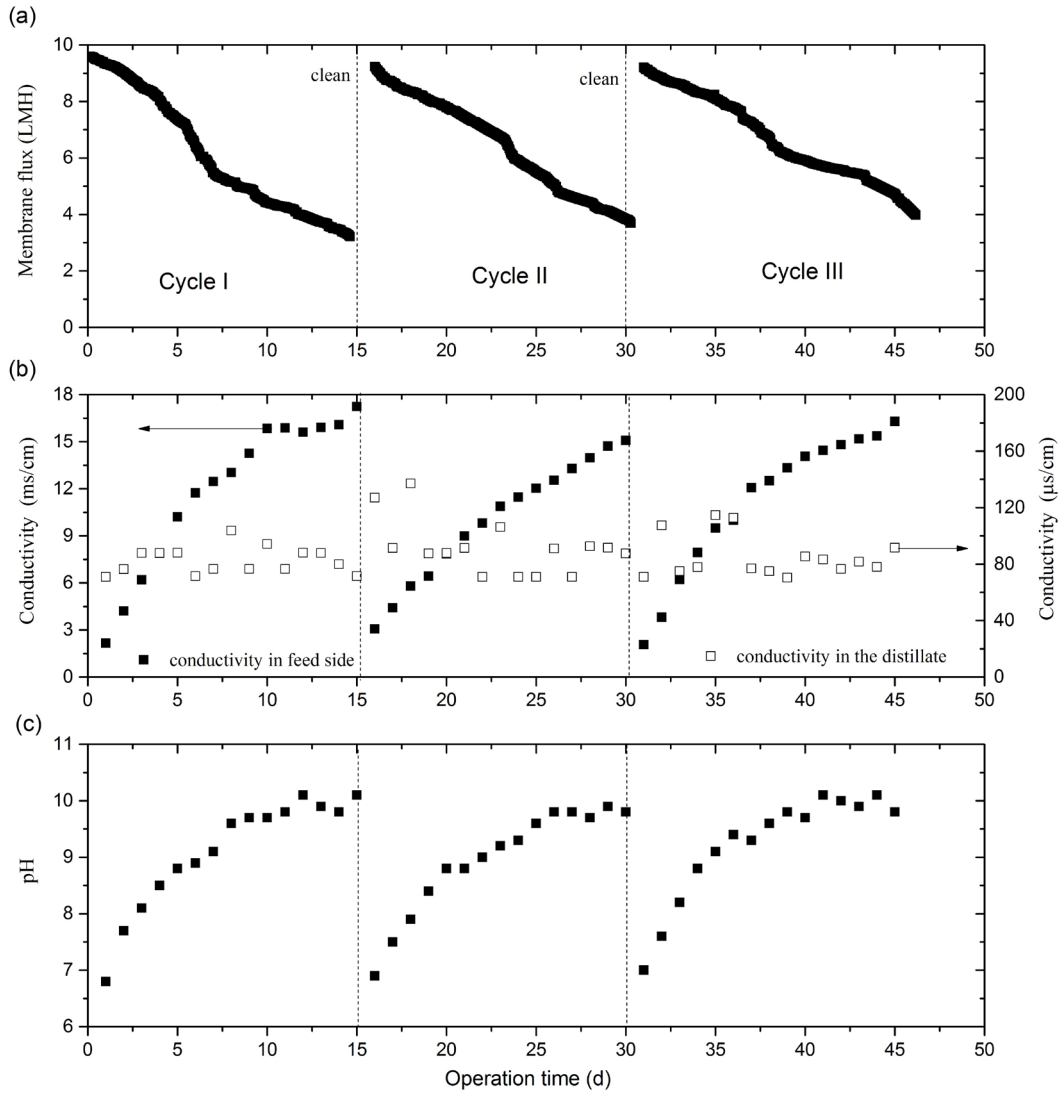

Fig. 2. Changes of: (a) membrane flux, (b) conductivity, and (c) pH during long-term operation.

5 mg/L, was detected in the distillate, and the COD removal rate during the whole operation time remained above 98.7%. This result was consistent with that of Kim et al. [10] that MD treatment removed almost all of the organic components after fermentative treatment, possibly due to vapor transport action compared with isothermal filtration showing 28%–87% retention ability (for a micro-porous membrane). Additionally, it was noteworthy that membrane cleaning did not alter rejection efficiency.

The detection of COD in the permeate might be related to the transport of volatile organic compounds and subtle membrane wetting. The VFAs normally exist in the volatile and non-volatile forms, depending on pH condition. Similarly to water vapor, VFA in volatile form can diffuse through the membrane pores [20]. Additionally, membrane wetting promotes COD in the distillate side. The membrane was weakened due to membrane wetting; therefore, the mass transfer resistance decreased, and partial organic matter passed through the pores leaving a small amount of COD [21]. This was confirmed by the detection of protein and polysaccharides in the permeate as shown in Figs. 3(b) and (c).

Polysaccharides and protein are kinds of non-volatile organic macromolecule compounds and the major components of wastewater treatment effluent [22]. The MD rejection for these compounds can theoretically be as high as 100%. Due to membrane wetting [21], only a trace of protein and polysaccharides was detected in the distillate, with concentrations less than 0.34 and 0.58 mg/L, respectively.

A sharp increase of COD, protein, and polysaccharides in the feed side was observed during the initial phase of each run, likely due to membrane interception and feed concentration. The protein and polysaccharides can be as high as 139.5 and 76.8 mg/L, respectively, and white-brown deposit was found on glassware or on the wall used for feed storage. The high temperature can alter the tertiary structure of the protein, and some interior non-polar groups can become surface exposed, resulting in a reduction of solubility [23].

Additionally, heat denaturation acted to increase the viscosity of the protein, promoting its attachment on the glassware surface. This phenomenon was also reported by Gryta et al. [24], although the observed deposit was a grey-brown color.

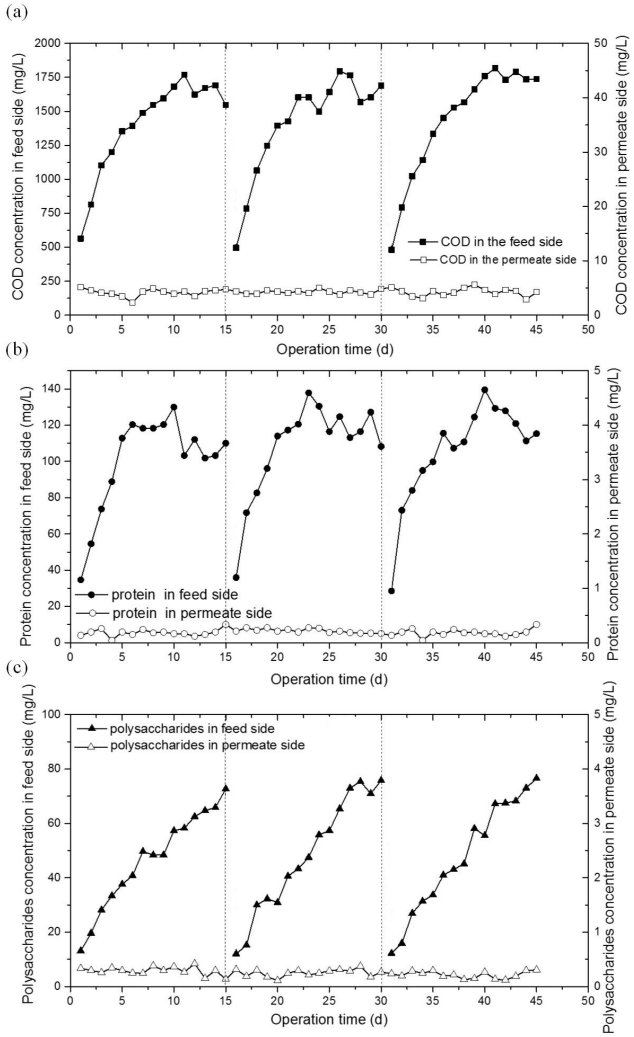

Fig. 3. Evolution of: (a) COD, (b) protein, and (c) polysaccharides concentrations in the feed and permeate side.

3.2.2. Phosphate variation over operation time

The variation of phosphate with operation time in the feed and distillate side is demonstrated in Fig. 4(a). With an inflow of 2.3 ± 0.3 mg/L, it was hard to detect PO_4^{3-}–P in the permeate side suggesting that the MD system was effective at phosphate removal. On the feed side, the accumulation of PO_4^{3-}–P in the initial phase was observed for each run followed by a decrease in concentration, and the membrane cleaning did not appear to affect the efficiency of phosphate interception. Looking at the first run, the concentration of PO_4^{3-}–P in the feed side first increased from 2.6 to 9.8 mg/L in 6 d and then decreased to around 5.5 mg/L. The concentration decline was likely attributed to the oversaturation and precipitation of phosphate since it was at sufficiently high concentration, and the pH increased to nearly 10. Considering the high interception property of the membrane, Ca, Mg, and P were effectively rejected, leading to the formation of scaling (e.g., $Ca_3(PO_4)_2$) as observed previously. The similar phenomenon was reported by other researches [25,26]. For example, Chen et al. [26] investigated phosphate decrease in a forward osmosis–AnMBR system, and suggested it might be attributed to precipitate in the form of amorphous calcium phosphate ($Ca_3(PO_4)_2$) or dicalcium phosphate dihydrate ($Ca_2H_2(PO_4)_2$).

Consistent removal of phosphorus to achieve the necessary standard of wastewater discharge is difficult only for biological treatment; thus, the addition of flocculants (e.g., $FeCl_3$, $Al_2(SO_4)_3$, CaO) is often required, leading to residual sludge production (due to secondary pollutants) and high operating costs. Here, the MD process is considered to be a promising and efficient technology to reduce effluent phosphorus, especially for eutrophication control.

3.2.3. Changes of NH_4^+–N over operation time

The variation of ammonia concentration in the feed and distillate side is shown in Fig. 4(b). With an inflow NH_4^+–N concentration of 33.2 ± 1.7 mg/L, its concentration in the feed side gradually decreased from 22.2 ± 1.2 to 10.1 ± 1.7 mg/L during each run. This is likely due to the stripping of ammonia under high temperature and pH. Generally, ammonia ions (NH_4^+) exist in equilibrium with ammonia (NH_3) according to Eq. (2), and most the ammonia would be soluble ammonia ions at pH values below 7 and would be dissolved

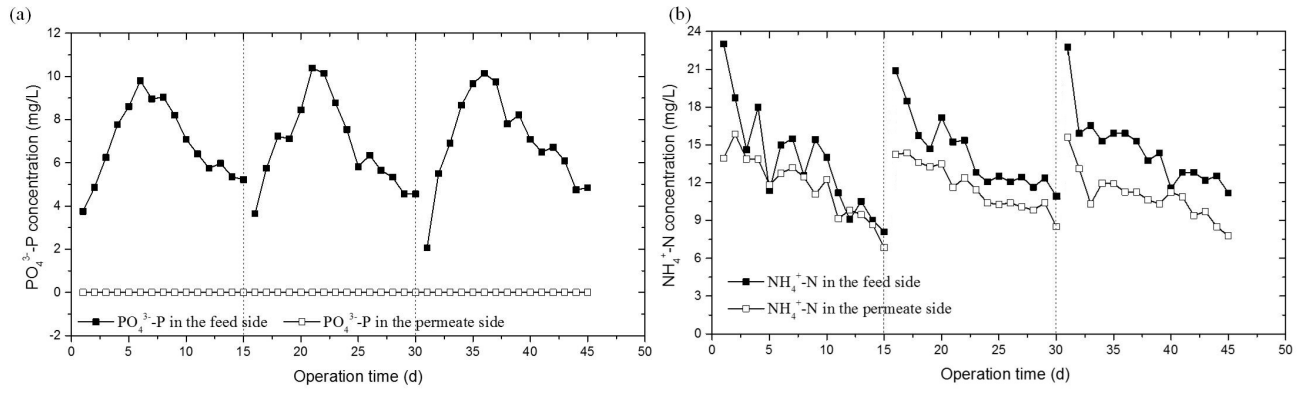

Fig. 4. (a) Changes of PO_4^{3-}–P and (b) evolution of NH_4^+–N against operation time in the feed and permeate.

gas at pH levels above 12. Higher temperature and pH favor the removal of ammonia from solution. The stripping rate of ammonia is significantly affected by its vapor pressure and saturated concentration, which is mainly dependent on the temperature [12]. Considering the high temperature in the feed side, the saturated concentration decreased, and vapor pressure increased according to Henry's law, resulted in an increase in the amount of free ammonia removed during the aqueous phase. Additionally, the high pH on the feed side promoted a right shift in the equilibrium (Eq. (2)), causing most ammonia to be in the NH_3 form especially later in each run, resulting in decreased concentration on the feed side. Ding et al. [27] reported that the pH of the feed side played a significant role in the ability of ammonia to pass through the MD membrane.

$$NH_4^+ + OH^- \rightleftarrows NH_3 + H_2O \quad (2)$$

Additionally, the concentration of NH_4^+–N in the distillate side was only slightly lower than that in the feed side, and followed the same trend. As the vapor pressure of ammonia was many orders of magnitude higher than that of the water molecules, the ammonia easily passed through the hydrophobic membrane, allowing a relative balance in ammonia on the feed and distillate side. A hybridization of MD process with an ammonia removal process might be utilized to remove the additional ammonia remaining after the MD process to improve this strategy for sustainable wastewater treatment. For example, stripping is a common strategy to remove volatile compounds from a wide variety of water source (Kim et al. [10]). Increasing temperature is another technology that promotes the free ammonia stripping from the liquid phase.

3.3. EEM analysis for feed and permeate

To further understand the characteristics of feed and permeate, EEM was employed to identify the changes of chemical components other than the polysaccharides. The EEM spectra of feed with the operation time are shown in Figs. 5(a)–(g). EEM fingerprints showed the dominant appearance of fluorophores consistent with tryptophan-like proteins (peak A) and humic-like materials (peak B) in the spectra of all the feed side samples. An additional, less distinct peak was assigned to fulvic components. During the 15-d interval, a gradual increase of fluorescence intensity was observed, especially for the humic-like acids. Quantification by the colorimetric method confirmed the same change of protein concentrations. The lower concentration ratio of tryptophan-like proteins compared with the humic-like fractions was consistent with the higher temperature degrading the protein. Additionally, the MD treatment allowed nearly complete removal of the fluorescent organic constituents as shown in Fig. 5(h), for all identified peak regions.

The other fluorophores related to tryptophan protein-like substances, aromatic protein-like substances, and fulvic acids were detected by EEM. However, the fluorescence was small, and it was difficult to locate the exact peak location and peak maxima. To further explore the composition changes in the feed side with the operation time, fluorescence regional integration (FRI) was used to analyze the six excitation–emission regions [28,29], including the region of tyrosine (I), tyrosine-like proteins (II), tryptophan (III), tryptophan-like proteins (IV), fulvic acid-like (V), and humic acid-like substances (VI). The feed side distribution of FRI is shown in Fig. 6. The feed bulk showed fluorescence in regions II, III, IV, and VI. Signal for region I accounted for less than 6.8%, while the sum of regions II, III, and IV accounted for more than 74.2%, indicating that the majority of proteins in the original feed were tyrosine-like, tryptophan, and tryptophan-like proteins. Additionally, region VI, representing the humic acid-like materials, only accounted for 13.9% in the original feed. However, there were different changing trends during the course of operation. No significant changes were detected for regions I and V, but there was an obvious decrease in tyrosine-like protein from 21.7% to 7.7%, and a slight decrement in tryptophan from 16.3% to 8.9% was observed with increased operation time. Conversely, regions IV and VI increased with the operation time, with the tryptophan-like proteins increasing from 35.2% to 45.2% in 7 d and stabilizing around 46.8%. The humic acid-like substances increased from

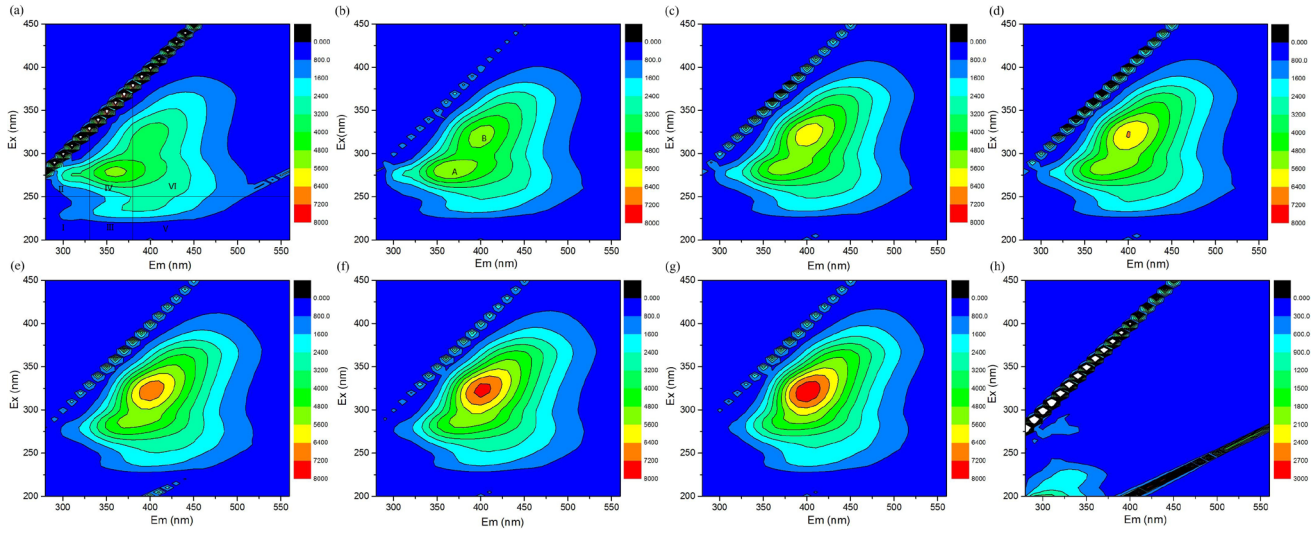

Fig. 5. EEM fluorescence spectra of: (a)–(g) feed at different time and (h) permeate.

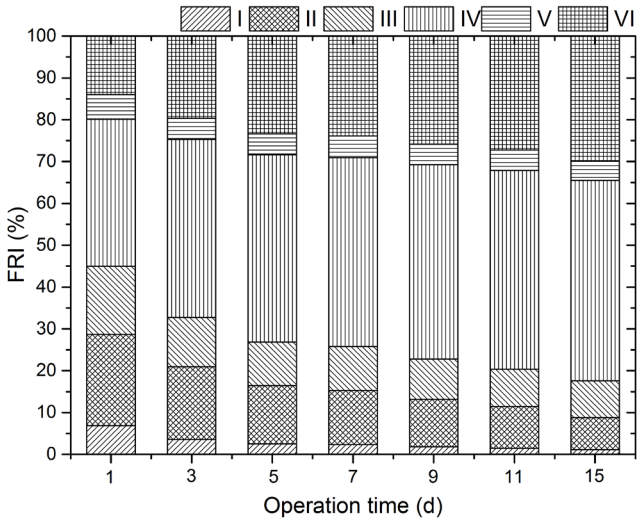

Fig. 6. FRI distribution of feed at different sampling time.

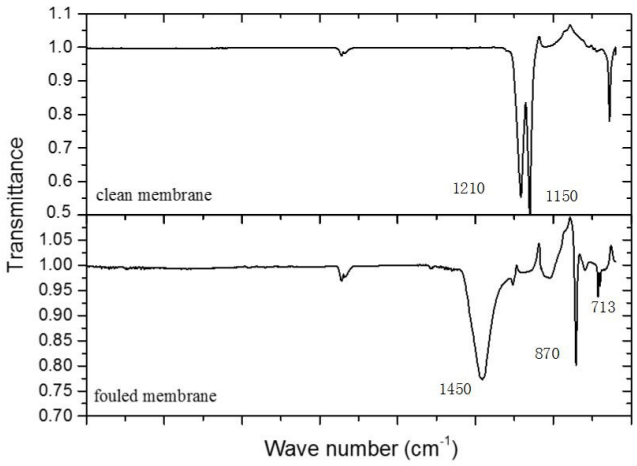

Fig. 7. ATR-FTIR spectra of clean and fouled membrane.

14.0% to 29.5% through each run. These measurements of protein and humic acid in the feed side were similar to those reported previously [30]. More importantly, the increase was greater for humic-like substances than that observed for protein materials, implying that the protein fraction was more sensitive to temperature degeneration and the humic fraction was more refractory toward this degradation. The protein in the feed side was likely underwent conformational change and denaturation by the unfolding of hydrophobic residues [31], loss of polar contacts, and increase of hydrophobic interaction [23], leading to deproteinization and precipitation and decreasing protein levels in the feed side.

3.4. Fouling investigation of distilled membrane

For MD and other membrane processes, fouling of the membrane surface leads to decreased membrane permeability and decreased efficiency. Fouling can result from the chemical reaction of solutes at the membrane boundary layer, inorganic scaling, organic compounds adsorption, and other causes [17]. In this study, the composition and morphology of the fouling layer were analyzed using ATR-FTIR and SEM–energy-dispersive X-ray spectroscopy (EDX).

The FTIR spectra of clean and fouled membranes are shown in Fig. 7. Two distinctive bands of C–F stretching vibrations at 1,150 and 1,220 cm^{-1} were clearly exhibited in the spectra of clean PTFE membrane [32]. These two peaks disappeared in the fouled membrane, and peaks contributed to v_3-asymmetric stretching (1,450 cm^{-1}), v_2-out-of-plane bending (870 cm^{-1}) vibrations of CO_3 group, and v_4-in-plane bending (713 cm^{-1}) vibration of CO_2 group were observed. These peaks were located in the same positions as they were in the spectrum of $CaCO_3$ (at 1,450, 870, and 713 cm^{-1}, spectrum from NIST Standard Reference Data), suggesting the presence of $CaCO_3$ in the fouling layer. The higher intensity of the absorption bands in the v_2–CO_3 and v_3–CO_3 domains revealed the presence of a calcium carbonate compound [33]. Hariharan et al. [34] pointed out that the sharp peak at 870 cm^{-1} indicated that the $CaCO_3$ obtained from the membrane surface was mostly in the form of calcite. More importantly, the peaks attributed to the protein structure (including amides I, C–O stretching; amides II, N–H in plane; and amides III, C–N stretching), polysaccharide-like substance (C–O bonds), and humic acids (carboxyl group) were not identified in the ATR-FTIR image, although these peaks are frequently observed on microfiltration (or ultrafiltration, RO) membrane during the filtration of wastewater treatment effluent. Therefore, it could be found that the decline of membrane flux was mainly resulted from $CaCO_3$ precipitation on the membrane surface and/or pores.

The SEM observation at the end of the experiment confirmed that the membrane surface was largely covered by deposit, leading to reduced membrane permeability (Fig. 8). The fouling deposit was analyzed by EDS which revealed that in addition to a large amount of Ca, the deposit also contained C, O, Mg, and P at atomic percentages of 18.75% (C), 24.32% (Ca), 50.86% (O), 1.69% (Mg), and 0.71% (P). Because Ca, C, and O were the major constituents of the fouling layer, the decrement of permeate was mostly contributed to $CaCO_3$ precipitation. Gryta [17] also reported that $CaCO_3$ deposition accumulated on the membrane surface. However, no simple explanation was provided for this scaling process, which was critically dependent on the feed concentration, temperature, residence time, and the flow condition (such as cross-flow velocity, flow chamber). The formation of deposit generally started in the largest pores, because they more rapidly underwent wettability [35]. When the wetted pores were over-filled, the supersaturation state enabled nucleation and crystal growth due to water evaporation and temperature changes [35,36]. Considering the minimum temperature for the formation of $CaCO_3$ at 40°C, the HCO_3^- ions present in the feed with 70°C underwent decomposition [19] allowing a large amount of $CaCO_3$ to precipitate on the membrane surface. Once the solute solubility decreased, the deposit can form quickly due to temperature polarization [36]. Other factors such as the extent of supersaturation, heat transfer rate, the condition of heat transfer surface, and the rate of carbon dioxide evolution can also contribute, as Pokrovsky [37] found that the scaling intensity increased with increased factor concentration. Mitigation approaches to eliminate precipitate formation included the acidification of feed to pH ~ 4, addition of anti-scalants, heat

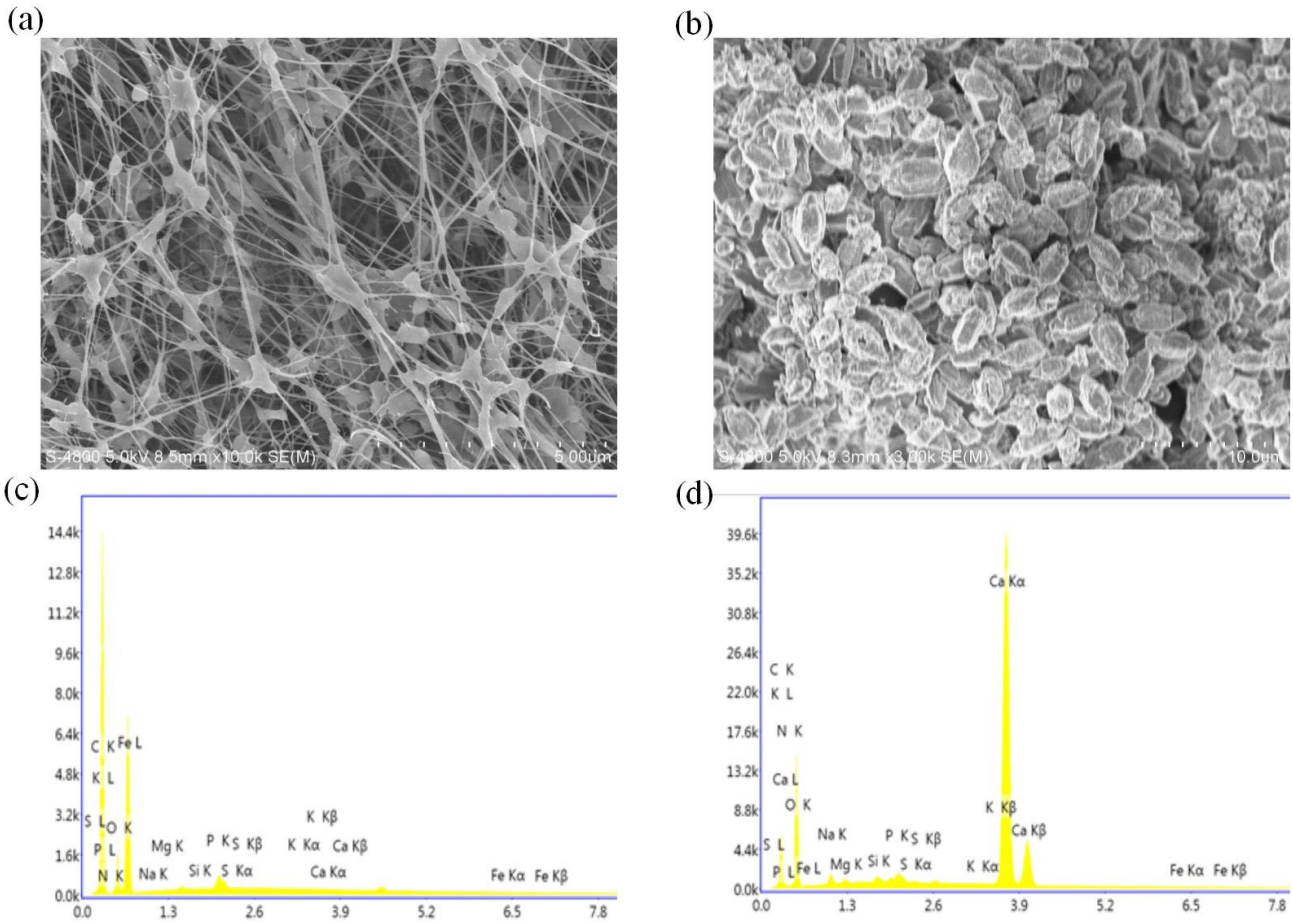

Fig. 8. (a) SEM of clean membrane, (b) SEM of fouled membrane, (c) EDX observation of clean membrane, and (d) EDX observation of fouled membrane.

pretreatment, and process optimization, though most of these were described for synthetic water. Thus, the selection of the most effective anti-scaling method to reduce membrane fouling should be investigated more fully.

3.5. Challenges

Compared with other membrane-based technology, the main advantages of MD include [2]: (1) complete rejection of macromolecules, ions, and other molecules; (2) lower operating pressures; (3) lower mechanical requirements for the membrane; and (4) lower operating temperature compared with conventional distillation. Additionally, membrane cleaning using citric acid and HCl did not cause adverse effects on organics/inorganics interception, exhibiting the promise of membrane cleaning as a strategy to allow long-term usage. However, many challenges remain, such as membrane fouling control and concentrated feed disposal.

The major problems of the MD process are related to membrane wetting and the formation of a fouling layer on membrane surface. The fouling and scaling accelerated the wetting process; thus, further investigation is required to more fully understand these phenomena. Considerable physiological challenges would be expected with increasing conductivity, such as due to polarization. For concentrated feed, a discharge with a high concentration of metal ions (Ca, Mg, etc.) would likely limit the reuse extent. Hence, the following aspects should be addressed in future work:

- development of new membrane and optimization of operating conditions to decrease fouling and extend membrane function;
- selecting the appropriate cleaning procedure and chemicals to extend the lifetime of membrane;
- elucidation of fouling mechanisms, and alleviation of scaling effects on membrane performance; and
- reasonable disposal of concentrated feed, especially ammonia removal for the produced distillate.

4. Conclusions

MD was successfully operated for AnMBR effluent treatment, and the following conclusions were obtained:

- MD showed very good separation of the AnMBR effluent for protein, polysaccharides, phosphate, and metal ions, while its performance was limited for volatile foulants like ammonia.

- Scaling inhibited the MD process, and the formation of mainly the $CaCO_3$-containing deposit on the membrane surface reduced membrane flux and might promote subtle wettability.
- Membrane permeate was recovered up to 94% of the initial flux by cleaning with a solution of 0.8 wt% critical acid + 0.3 wt% HCl with no obvious difference in membrane interception efficiency.

Acknowledgments

This study was mainly financially supported by Natural Science Fund of Jiangsu (grant number: BK20150813), National Natural Science Fund of China (grant number: 51508153), Fundamental Research Funds for the Central Universities, and a project funded by the Priority Academic Program Development of Jiangsu Higher Education Institutions.

References

[1] M.A. Shannon, P.W. Bohn, E. Menachem, J.G. Georgiadis, B.J. Marinas, A.M. Mayes, Science and technology for water purification in the coming decades, Nature, 452 (2008) 301–310.
[2] B.L. Pangarkar, S.K. Deshmukh, V.S. Sapkal, R.S. Sapkal, Review of membrane distillation process for water purification, Desal. Wat. Treat., 57 (2014) 1–23.
[3] B.L. Pangarkar, M.G. Sane, S.B. Parjane, M. Guddad, Status of membrane distillation for water and wastewater treatment—a review, Desal. Wat. Treat., 52 (2014) 5199–5218.
[4] J.B. Rodríguez, V.M. Gabet, G.M. Monroy, A.B. Puerta, I.F. Barrio, Distilled and drinkable water quality produced by solar membrane distillation technology, Desal. Wat. Treat., 51 (2013) 1265–1271.
[5] M. Osman, J.J. Schoeman, L. Baratta, Desalination/concentration of reverse osmosis and electrodialysis brines with membrane distillation, Desal. Wat. Treat., 24 (2010) 293–301.
[6] S. Lee, Y. Kim, A.S. Kim, S. Hong, Evaluation of membrane-based desalting processes for RO brine treatment, Desal. Wat. Treat., 57 (2016) 7432–7439.
[7] K. Bélafi-Bakó, A. Boór, Concentration of Cornelian cherry fruit juice by membrane osmotic distillation, Desal. Wat. Treat., 35 (2011) 271–274.
[8] N. Mokhtar, W. Lau, B. Ng, A. Ismail, D. Veerasamy, Preparation and characterization of PVDF membranes incorporated with different additives for dyeing solution treatment using membrane distillation, Desal. Wat. Treat., 56 (2015) 1999–2012.
[9] M. Sivakumar, M. Ramezanianpour, G. O'Halloran, Mine water treatment using a vacuum membrane distillation system, APCBEE Procedia, 5 (2013) 157–162.
[10] H.-C. Kim, J. Shin, S. Won, J.-Y. Lee, S.K. Maeng, K.G. Song, Membrane distillation combined with an anaerobic moving bed biofilm reactor for treating municipal wastewater, Water Res., 71 (2015) 97–106.
[11] H. Liu, J. Wang, Treatment of radioactive wastewater using direct contact membrane distillation, J. Hazard. Mater., 261 (2013) 307–315.
[12] P. Jacob, P. Phungsai, K. Fukushi, C. Visvanathan, Direct contact membrane distillation for anaerobic effluent treatment, J. Membr. Sci., 475 (2015) 330–339.
[13] E.W. Rice, L. Bridgewater, Standard Methods for the Examination of Water and Wastewater, American Public Health Association, Washington, D.C., 2012.
[14] M. Dubois, K.A. Gilles, J.K. Hamilton, P.A. Rebers, F. Smith, Colorimetric method for determination of sugars and related substances, Anal. Chem., 28 (1956) 350–356.
[15] B. Frolund, T. Griebe, P.H. Nielsen, Enzymatic activity in the activated-sludge floc matrix, Appl. Microbiol. Biotechnol., 43 (1995) 755–761.
[16] M. Gryta, Influence of polypropylene membrane surface porosity on the performance of membrane distillation process, J. Membr. Sci., 287 (2007) 67–78.
[17] M. Gryta, Fouling in direct contact membrane distillation process, J. Membr. Sci., 325 (2008) 383–394.
[18] L.D. Nghiem, F. Hildinger, F.I. Hai, T. Cath, Treatment of saline aqueous solutions using direct contact membrane distillation, Desal. Wat. Treat., 32 (2011) 234–241.
[19] E. Drioli, E. Curcio, A. Criscuoli, G.D. Profio, Integrated system for recovery of $CaCO_3$, NaCl and $MgSO_4 \cdot 7H_2O$ from nanofiltration retentate, J. Membr. Sci., 239 (2004) 27–38.
[20] K. Karakulski, M. Gryta, Water demineralisation by NF/MD integrated processes, Desalination, 177 (2005) 109–119.
[21] J. Kochan, T. Wintgens, R. Hochstrat, T. Melin, Impact of wetting agents on the filtration performance of polymeric ultrafiltration membranes, Desalination, 241 (2009) 34–42.
[22] D.J. Barker, D.C. Stuckey, A review of soluble microbial products (SMP) in wastewater treatment systems, Water Res., 33 (1999) 3063–3082.
[23] Y. Zhao, F. Li, M.T. Carvajal, M.T. Harris, Interactions between bovine serum albumin and alginate: an evaluation of alginate as protein carrier, J. Colloid Interface Sci., 332 (2009) 345–353.
[24] M. Gryta, M. Tomaszewska, J. Grzechulska, A.W. Morawski, Membrane distillation of NaCl solution containing natural organic matter, J. Membr. Sci., 181 (2001) 279–287.
[25] A. Trzcinski, D. Stuckey, Continuous treatment of the organic fraction of municipal solid waste in an anaerobic two-stage membrane process with liquid recycle, Water Res., 43 (2009) 2449–2462.
[26] L. Chen, Y. Gu, C. Cao, J. Zhang, J.W. Ng, C. Tang, Performance of a submerged anaerobic membrane bioreactor with forward osmosis membrane for low-strength wastewater treatment, Water Res., 50 (2014) 114–123.
[27] Z. Ding, L. Liu, Z. Li, R. Ma, Z. Yang, Experimental study of ammonia removal from water by membrane distillation (MD): the comparison of three configurations, J. Membr. Sci., 286 (2006) 93–103.
[28] W. Chen, P. Westerhoff, J.A. Leenheer, K. Booksh, Fluorescence excitation–emission matrix regional integration to quantify spectra for dissolved organic matter, Environ. Sci. Technol., 37 (2003) 5701–5710.
[29] Y. Li, A.-M. Li, J. Xu, W.-W. Li, H.-Q. Yu, Formation of soluble microbial products (SMP) by activated sludge at various salinities, Biodegradation, 24 (2013) 69–78.
[30] G. Naidu, S. Jeong, S.-J. Kim, I.S. Kim, S. Vigneswaran, Organic fouling behavior in direct contact membrane distillation, Desalination, 347 (2014) 230–239.
[31] H. Mo, K.G. Tay, H.Y. Ng, Fouling of reverse osmosis membrane by protein (BSA): effects of pH, calcium, magnesium, ionic strength and temperature, J. Membr. Sci., 315 (2008) 28–35.
[32] F. Wang, H. Zhu, H. Zhang, H. Tang, J. Chen, Y. Guo, Effect of surface hydrophilic modification on the wettability, surface charge property and separation performance of PTFE membrane, J. Water Process Eng., 8 (2015) 11–18.
[33] C. Combes, R. Bareille, C. Rey, Calcium carbonate-calcium phosphate mixed cement compositions for bone reconstruction, J. Biomed. Mater. Res., A, 79 (2006) 318–328.
[34] M. Hariharan, N. Varghese, A.B. Cherian, P.V. Sreenivasan, J. Paul, K.A. Asmy Antony, Synthesis and characterisation of $CaCO_3$ (Calcite) nano particles from cockle shells using chitosan as precursor, Int. J. Sci. Res. Publ., 4 (2014) 1–5.
[35] A.M. Alklaibi, N. Lior, Membrane-distillation desalination: status and potential, Desalination, 171 (2005) 111–131.
[36] F. He, J. Gilron, H. Lee, L. Song, K.K. Sirkar, Potential for scaling by sparingly soluble salts in crossflow DCMD, J. Membr. Sci., 311 (2008) 68–80.
[37] O.S. Pokrovsky, Precipitation of calcium and magnesium carbonates from homogeneous supersaturated solutions, J. Cryst. Growth, 186 (1998) 233–239.